Available online at www.sciencedirect.com
SCIENCE DIRECT®
Journal of Solid State Chemistry 178 (2005) 1440–1444
JOURNAL OF SOLID STATE CHEMISTRY
www.elsevier.com/locate/jssc

Growth of high quality and large-sized $Rb_{0.3}MoO_3$ single crystals by molten salt electrolysis method

Junfeng Wang[a,*], Rui Xiong[a], Fan Yi[a], Di Yin[a], Manzhu Ke[a], Changzhen Li[a], Zhengyou Liu[a], Jing Shi[a,b]

[a]*Department of Physics, Wuhan University, Wuhan 430072, China*
[b]*International Center for Material Physics, Shenyang 110015, China*

Received 18 October 2004; received in revised form 14 February 2005; accepted 15 February 2005
Available online 17 March 2005

Abstract

High quality and large-sized $Rb_{0.3}MoO_3$ single crystals were synthesized by molten salt electrolysis method. X-ray diffraction (XRD) patterns and rocking curves, as well as the white beam Laue diffraction of X-ray images show the crystals grown by this method have high quality. The lattice constants evaluated from XRD patterns are $a_0 = 1.87$ nm, $b_0 = 0.75$ nm, $c_0 = 1.00$ nm, $\beta = 118.83°$. The in situ selected area electron diffraction (SAED) patterns along the $[10\bar{1}]$, $[1\bar{1}\bar{1}]$ and $[10\bar{3}]$ zone axes at room temperature indicate that the $Rb_{0.3}MoO_3$ crystal possess perfect C-centered symmetry. Temperature dependence of the resistivity shows this compound undergoes a metal to semiconductor transition at 183 K.

PACS: 71.45.Lr; 81.10.Eq

Keywords: Blue bronze $Rb_{0.3}MoO_3$; Single crystal growth; Electrolytic reduction; Charge density wave

1. Introduction

During the past decades, much attention has been paid to a class of quasi-one-dimensional oxides known as the molybdenum blue bronzes with the generic chemical form $A_{0.3}MoO_3$ ($A = K$, Rb, or Tl) [1–6]. The structure of these compounds consists of infinite chains of distorted MoO_6 octahedra with sharing corners along the monoclinic [010] direction [1–3]. Owing to this highly anisotropic layered structure, blue bronzes exhibit a charge-density-wave (CDW) instability below a Peierls temperature T_p, which results in a transition from metal to semiconductor behavior. If an electric field is applied beyond a certain threshold field, charge is transported with the sliding of the density wave. This CDW transport leads to many interesting phenomena such as strongly nonlinear conduction, coherent current oscillations, and mode locking at resonant frequencies [4–6].

Recently, van der Zant et al. [7–9] successfully fabricated a thin-film of the oxide $Rb_{0.3}MoO_3$ by pulsed-laser deposition (PLD). This makes the practical device applications of CDW materials possible. However, because of the lower melting point for Rb_2MoO_4 and MoO_3 as starting materials, it is difficult to prepare high-quality polycrystalline single-phase $Rb_{0.3}MoO_3$ target-materials by conventional solid reaction method under normal pressure. Therefore, high quality and large-sized $Rb_{0.3}MoO_3$ single crystals are important and necessary for the further investigation on the mechanism of CDW transport and application, especially as target-materials for the preparation of CDW films. Up to now, there are two methods for $A_{0.3}MoO_3$ single crystal growth: the gradient flux technique and the electrolytic reduction method. Collins et al. [10], by means of the

*Corresponding author. Fax: +86 27 6875 2569.
E-mail address: janson_iris@163.com (J. Wang).

0022-4596/$ - see front matter © 2005 Elsevier Inc. All rights reserved.
doi:10.1016/j.jssc.2005.02.015

gradient flux technique, grew $Tl_{0.3}MoO_3$ single crystals with Tl_2MoO_4, MoO_3 and MoO_2 as raw materials (Ganne et al. also grew $Tl_{0.9}Mo_6O_{17}$ by this method [11]). Ghedira et al. [12] grew $A_{0.3}MoO_3$ single crystals with A_2MoO_4 ($A = K$, Rb) and MoO_3 as starting materials by means of the electrolytic reduction method, but no details were given. The typical dimensions of the obtained single crystals for these two groups were $3 \times 1.5 \times 1\,mm^3$ by the gradient flux technique [10] and $5 \times 2 \times 1\,mm^3$ by the electrolytic reduction method [12], respectively. In this paper, we report an improved electrolytic reduction method by changing the starting materials and the conditions of crystal growth. Although the synthesis of the rubidium molybdenum bronze by molten salt electrolysis is not new, we provide details not heretofore published. Furthermore, the as-synthesized $Rb_{0.3}MoO_3$ single crystals in this work have large average size $10 \times 4 \times 3\,mm^3$ and high quality determined by X-ray diffraction using the white beam Laue diffraction and rocking techniques, as well as electrical transport measurements.

2. Experiments

The crystal growth of rubidium blue bronze was performed in an electrolytic cell shown in Fig. 1. The melt was contained in a 100-mL high-purity alumina crucible, which was seated in the bottom of the vertical tubular furnace. The cathode was made of a 1.2 mm dia. platinum wire, and the anode was made of a $10 \times 10\,mm^2$ platinum plate. Both the cathode and anode were placed in a long quartz tube and were centered in the tube with an inner cylindrical compartment. The quartz tube with the platinum electrodes could be raised or lowered into the crucible by a special guide.

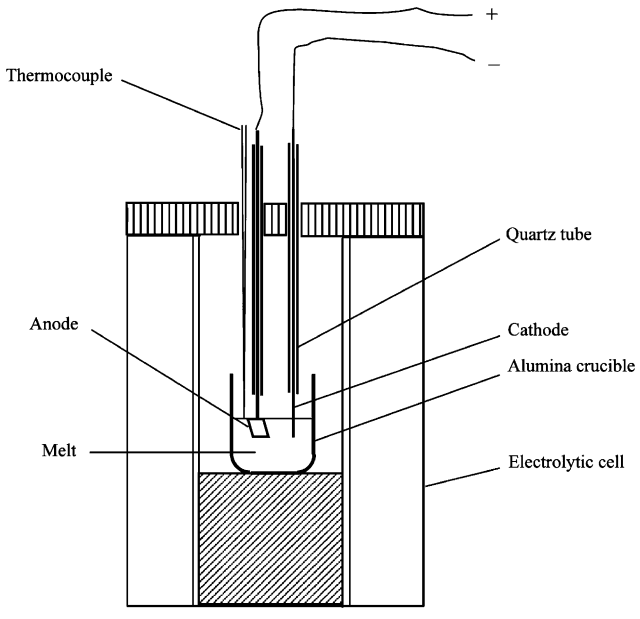

Fig. 1. Electrolytic cell for crystal growth of molybdenum bronzes.

In Ref. [12], the molten salts were the mixtures of Rb_2CO_4 and MoO_3 with mole ratio 1:3.35. In this work, we used Rb_2CO_3 and MoO_3 as starting materials with mole ration around 1:4.3. In a typical electrolysis run, the sample charge (60–80 g) was intimately mixed and placed in the crucible. The mixtures of Rb_2CO_3 and MoO_3 were reacted and melted in the crucible in a dry atmosphere at 590 °C for 12 h. Then the temperature was brought to a temperature slightly above the melting point. The cathode and anode were lowered about 10 mm below the melt surface, and the electrolysis current was controlled between 20 and 40 mA to pass through the melt for 2–3 h. At the end of the process, the quartz tubes and the electrodes were raised above the melt and the blue crystals of molybdenum bronzes were found on the cathode. They were recovered by soaking them in hot dilute HCl. The process of crystal growth can be repeated many times and can last more than 12 days if the mixtures of the starting materials are about 80 g in weight.

In a typical electrolysis run, the reaction process is described by:

$$3Rb_2CO_3 + 20MoO_3 \rightarrow 20Rb_{0.3}MoO_3 + 3CO_2\uparrow + 3/2O_2\uparrow$$

X-ray diffraction (XRD) data were collected on a D/Max-rA diffractometer using Cu$K\alpha$ radiation. The working voltage, current and time constant were 40 kV, 50 mA and 0.2 s, respectively. For rocking curve measurement, the working voltage and current were 40 kV and 10 mA, respectively.

The in situ selected area electron diffraction (SAED) observation was carried out in the JEOL JEM-2010 (HT) TEM at room temperature with thermionic electron gun (Brightness $\sim 5 \times 10^6\,A/cm^2\,sr$) and high tilt (HT) pole pieces.

The white beam Laue diffraction image using differential-aperture X-ray microscopy (DAXM) technique was taken at 34ID-E microdiffraction station in Advanced Photon Source, Argonne National Laboratory. The beamsize of the X-ray microbeam is $\sim 0.5\,\mu m$ diameter. The typical white beam energy range is 8–24 keV, which ensure that the X-rays have pass through our small thickness of sample. An area detector (CCD) is placed above sample to collect $\pm 40^\circ$ in 2θ angle.

Electrical resistivity was measured along the [010] direction by a conventional four-probe configuration. A gold film was vaporized on the two current terminals of the sample to assure good quality of contact. Copper wires were soldered to the gold film by silver paint to

ensure the homogeneous injection of current. Ohmic contacts to the crystals were obtained in such method. The whole system was entirely controlled by a computer and all the measurements were performed in ^{4}He cryostat over temperature from 250 to 74 K.

3. Results and discussion

The conditions and results of the electrolysis are summarized in Table 1. The formation and crystal growth were mainly dependent on the temperature, melt composition and electrolysis current density. In these systems, lower temperatures were found to improve product yields, thus melt temperature was generally held just above the solidification temperature. Large and high-quality single crystals of blue bronze could be obtained when the percentage of Rb_2CO_3 was between 18 and 20 mol% and the temperature was controlled between 570 and 590 °C. The typical size of rubidium blue bronze grown in our experiments was a prism with dimensions of $10 \times 4 \times 3\,mm^3$. The largest one we obtained had dimensions of $15 \times 5.5 \times 1.8\,mm^3$ (Fig. 2).

Fig. 3 shows X-ray diffraction (XRD) patterns of $Rb_{0.3}MoO_3$ grown by this method. No trace of an additional phase is found in XRD patterns in Fig. 3b, indicating the formation of single phase of $Rb_{0.3}MoO_3$ (we only labeled part of the diffraction peaks according to JCPDS-PDF-25-0733). Fig. 3a shows an XRD profile taken for the surface perpendicular to the plotting paper. All of diffraction peaks are assigned to be integer multiples of $\bar{2}01$ diffraction peak of the $Rb_{0.3}MoO_3$ phase, indicating this surface is the $(\bar{2}01)$ cleavage plane. Fig. 3c shows a rocking curve for $(\bar{2}01)$ plane. The full-width at half-maximum (FWHM) is approximately 0.2° for 40 kV working voltage and 10 mA current. The sharp peak and smooth background indicate that the crystals have high qualities. By the use of a C-centered unit cell with $\beta = 118.83°$ (JCPDS-PDF-25-0733), the lattice constants evaluated from XRD patterns are $a_0 = 1.87$ nm, $b_0 = 0.75$ nm, $c_0 = 1.00$ nm, which are in good agreement with those of Kohn et al. ($a_0 = 1.863$ nm, $b_0 = 0.755$ nm, $c_0 = 1.009$ nm, $\beta = 118.842°$) [13] and Schutte et al. ($a_0 = 1.853$ nm, $b_0 = 0.755$ nm, $c_0 = 1.003$ nm, $\beta = 118.52°$) [14], as well as the result of Ghedira et al. ($a_0 = 1.636$ nm, $b_0 = 0.755$ nm, $c_0 = 1.009$ nm) [12] obtained by translating the C-centered unit cell to an I-centered unit cell of equal volume with $\beta = 93.87°$.

Fig. 4 shows the white beam Laue diffraction of X-ray images of the as-prepared $Rb_{0.3}MoO_3$ single crystal. The sharpness of the Laue spots tells the quality of the sample, and the constant local orientation tells that this is a very good single crystal. We also made an energy scan on one of the reflection (fixed incident beam direction with changeable incident energy). This scan could give the intensity as a function of d-spacing, which is similar to the regular $\theta - 2\theta$ scan (fixed energy with changeable incident beam direction). This technique provides $<10^{-2}$ degrees angular resolution in local orientation determination and $<10^{-4}$ residual strain precision.

The SAED patterns of $Rb_{0.3}MoO_3$ along the $[10\bar{1}]$, $[1\bar{1}1]$ and $[10\bar{3}]$ zone axes at room temperature are shown in Fig. 5a–c. The patterns indicate that the $Rb_{0.3}MoO_3$ crystal possesses perfect C-centered symmetry. The reflections (111) in the $[10\bar{1}]$ SAED pattern and (311) in $[10\bar{3}]$ pattern shown in Fig. 5a and c denote the C-center symmetry.

Fig. 6 shows the temperature dependence of the resistivity of $Rb_{0.3}MoO_3$ single crystal along [010] direction. In order to make the transition temperature clear, we use the logarithmic axis for resistivity. The resistivity of $Rb_{0.3}MoO_3$ single crystal decreases linearly with temperature decreasing from 250 to 183 K, showing a good metallic behavior. At 183 K, a transition appears and the resistivity begins to increase significantly with

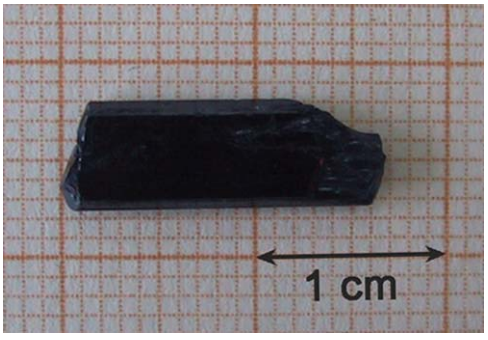

Fig. 2. A large $Rb_{0.3}MoO_3$ single crystal with dimensions of $15 \times 5.5 \times 1.8\,mm^3$. The [010] direction is parallel to the arrow.

Table 1
Conditions of the crystal growth in this work

Composition (mol%)	Temperature (°C)	Current (mA)	Duration (h)	Crystals obtained
Rb_2CO_3 (18–20%) MoO_3 (82–80)	570–590	20–40	2–3	Blue bronze $Rb_{0.3}MoO_3$
Rb_2CO_3 (23–24%) MoO_3 (77–76)	590–610	20–30	2–3	Red bronze $Rb_{0.33}MoO_3$

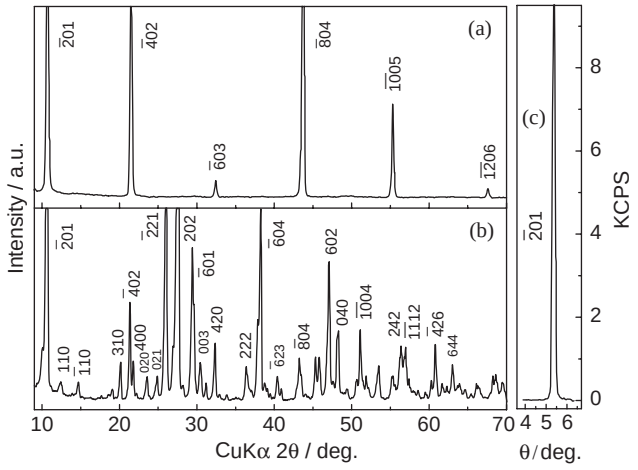

Fig. 3. X-ray diffraction patterns for as-synthesized $Rb_{0.3}MoO_3$ single crystals. (a) Diffraction pattern for the cleaved surface perpendicular to the growing axis. (b) Diffraction pattern for pulverized single crystals. (c) The rocking curve for $(\bar{2}01)$ surface. The working voltage and current are 40 kV and 10 mA, respectively.

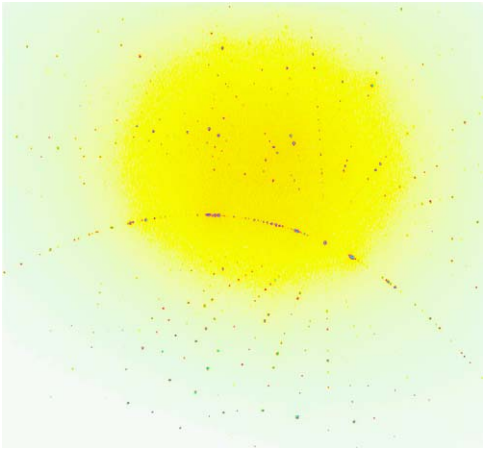

Fig. 4. The white beam Laue diffraction images of $Rb_{0.3}MoO_3$ single crystal.

decreasing temperature from 183 to 74 K. Regarding the experimental error of temperature measurement in different labs, our resistivity result is in agreement with that of the previous reported (the transition temperatures are 181, 183 and 180 K for the three compounds $A_{0.3}MoO_3$ ($A = K$, Rb, Tl), respectively) [10,15–17], which indicate that the Peierls transition of blue bronzes is not sensitive to the substitution of alkali metal ions and Tl element.

In conclusion, we have provided a detailed report on the growth of relatively large-sized $Rb_{0.3}MoO_3$ single crystals by an improved molten salt electrolysis method. XRD patterns and rocking curves, as well as the white beam diffraction of X-ray images show the crystals grown by this method have high quality. To date CDW films of $Rb_{0.3}MoO_3$ grown by means of PLD have utilized polycrystalline single-phase $Rb_{0.3}MoO_3$ targets. One may expect the quality of the $Rb_{0.3}MoO_3$ thin-film

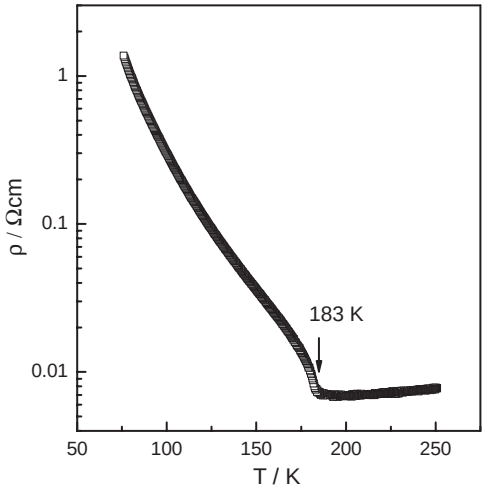

Fig. 6. Temperature dependence of the resistivity of as-prepared $Rb_{0.3}MoO_3$ single crystal along [010] direction.

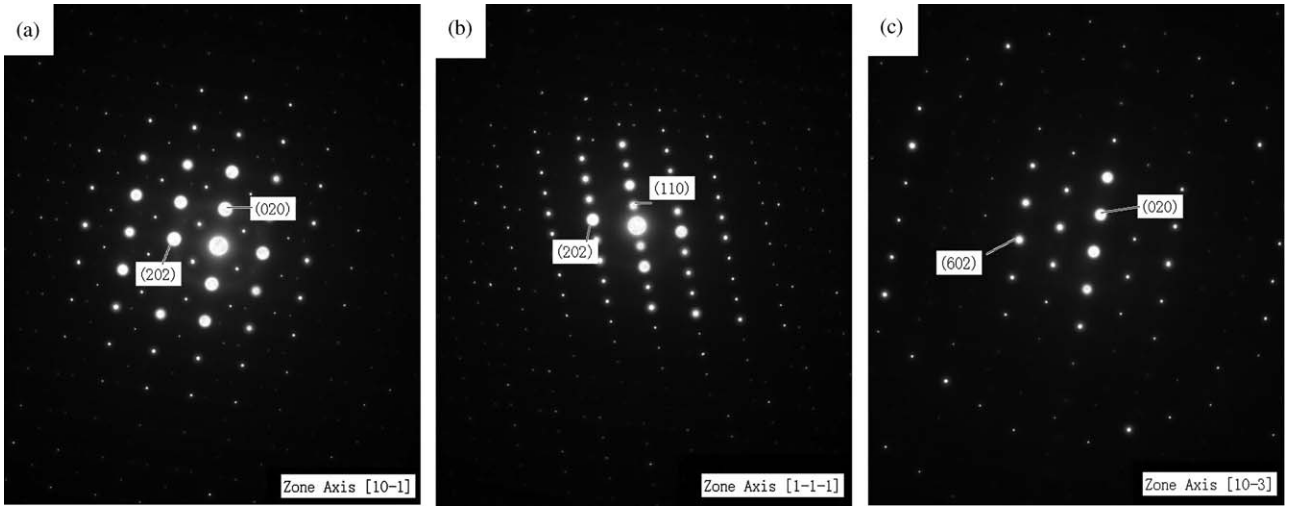

Fig. 5. The SAED patterns of $Rb_{0.3}MoO_3$ recorded along different zone axis at the room temperature. (a) $[10\bar{1}]$ (b) $[1\bar{1}\bar{1}]$ and (c) $[10\bar{3}]$.

would be better if these large-sized single crystals are used to substitute for the polycrystalline targets.

Acknowledgments

We thank Dr. W. Yang for the Laue diffraction test in this work. The X-ray Laue measurements were performed on UNICAT beamline at the Advanced Photon Source (APS), which is supported by the US Department of Energy, office of Science. This work was supported by the National Natural Science Foundation of China (No. 10474074) and State Key Laboratory of Advanced Technology for Materials Synthesis and Processing (Wuhan University of Technology) WUT 2004 M03.

References

[1] M. Greenblatt, Chem. Rev. 88 (1988) 31.
[2] G. Gruner, Rev. Mod. Phys. 60 (1988) 1129.
[3] C. Schenker (Ed.), Physics and Chemistry of Low-Dimensional Inorganic Conductors, Plenum Press, New York, 1996.
[4] J. Dumas, C. Schlenker, J. Marcus, R. Buder, Phys. Rev. Lett. 50 (1983) 757.
[5] J. Dumas, C. Schlenker, Int. J. Mod. Phys. B 7 (1993) 4045.
[6] B. Zawilski, J. Marcus, T. Klein, Europhys. Lett. 50 (2000) 75.
[7] H.S.J. van der Zant, O.C. Mantel, C. Dekker, J.E. Mooij, et al., Appl. Phys. Lett. 68 (1996) 3823.
[8] O.C. Mantel, H.S.J. van der Zant, A.J. Steinfort, C. Dekker, Phys. Rev. B 55 (1997) 4817.
[9] A.J. Steinfort, H.S.J. van der Zant, A.B. Smitts, O.C. Mantel, P.M.L.O. Scholte, C. Dekker, Phys. Rev. B 57 (1998) 12530.
[10] B.T. Collins, K.V. Ramanujachary, M. Greenblatt, J.V. Waszczak, Solid State Commun. 56 (1985) 1023.
[11] M. Ganne, M. Dion, A. Boumaza, M. Tournoux, Solid State Commun. 59 (1986) 137.
[12] M. Ghedira, J. Chenavas, M. Marezio, J. Marcus, J. Solid State Chem. 57 (1985) 300.
[13] W. Kohn, Phys. Rev. Lett. 19 (1967) 439.
[14] W.J. Schutte, J.L. de Boer, Acta Crystallogr. B 49 (1993) 579.
[15] R.M. Fleming, L.F. Schneemeyer, D.E. Moncton, Phys. Rev. B 31 (1985) 899.
[16] J. Dumas, C. Schlenker, J. Marcus, R. Buder, Phys. Rev. Lett. 50 (1983) 757.
[17] J. Dumas, A. Arbaoui, H. Guyot, J. Marcus, C. Schlenker, Phys. Rev. B 30 (1984) 2249.